

Robust entanglement generation by reservoir engineering

Christine A. Muschik¹, Hanna Krauter², Kasper Jensen², Jonas M. Petersen², J. Ignacio Cirac³, and Eugene S. Polzik²

¹ *ICFO-Institut de Ciències Fotòniques, Mediterranean Technology Park, 08860 Castelldefels (Barcelona), Spain.*

² *Niels Bohr Institute, Danish Quantum Optics Center QUANTOP, Copenhagen University, Blegdamsvej 17, 2100 Copenhagen, Denmark.*

³ *Max-Planck-Institut für Quantenoptik, Hans-Kopfermann-Str. 1, D-85748 Garching, Germany.*

Following a recent proposal [C. Muschik et. al., Phys. Rev. A **83**, 052312 (2011)], engineered dissipative processes have been used for the generation of stable entanglement between two macroscopic atomic ensembles at room temperature [H. Krauter et. al., Phys. Rev. Lett. **107**, 080503 (2011)]. This experiment included the preparation of entangled states which are continuously available during a time interval of one hour. Here, we present additional material, further-reaching data and an extension of the theory developed in [C. Muschik et. al., Phys. Rev. A **83**, 052312 (2011)]. In particular, we show how the combination of the entangling dissipative mechanism with measurements can give rise to a substantial improvement of the generated entanglement in the presence of noise.

I. INTRODUCTION

In a recent experiment [1, 2], a new technique for generating extremely robust and long-lived entanglement has been demonstrated following a proposal put forward in [3] (see also [4]). By means of reservoir engineering [5–26], entanglement has been produced purely dissipatively. Moreover, it has been shown how engineered dissipative processes in combination with continuous measurements can be used to create entanglement in a steady state. Using this method, entanglement between two macroscopic atomic ensembles [27] has been maintained and verified for up to one hour. This extends the time intervals during which event-ready entanglement of material objects can be provided by several orders of magnitude. In this article, we give an extended description of this experiment and present additional supporting data. A detailed and rigorous derivation of theoretical framework of the employed dissipative entangling mechanism can be found in [3]. Here, we also discuss an extension of this method which has been used in the experiment and includes measurements. We show how they can be used to improve the purely dissipative protocol and explain the basic working principle in detail.

The coupling of a quantum system to its environment, commonly referred to as dissipation, is traditionally considered to be a main problem impairing experiments involving quantum superposition states and the development of quantum technologies. Harnessing dissipative processes rather than aiming for eliminating their influence is a radically new concept and represents a paradigm shift in Quantum Information Science. We show that even limited control of the coupling between system and environment can enable one to turn a major problem into an asset. This change in perspective is not only of conceptual interest, but yields also significant practical advantages. The protocol discussed here relies on engineered dissipation. More specifically, the coupling of a system with a reservoir is tailored such that the desired state is obtained as the steady state of the dissipative

evolution. This way, the target state is reached independently of the initial conditions. Accordingly, this type of protocol does not require the precise initialization of the system in a well defined state. The resulting quantum state can be maintained for long times since it is stabilized by the dissipative dynamics. This mechanism continuously drives the system into the desired entangled state, even in the presence of noise sources, which limit the coherence time of the quantum system. Thus, the use of engineered dissipation enables the realization of unlimited entanglement lifetimes, which is not achievable by traditional methods.

We consider here two macroscopic atomic ensembles at room temperature interacting with freely propagating coherent light. Quantum information can be encoded in collective atomic spin states which are unaffected by the thermal motion of the atoms. This system has been shown to provide an excellent platform for quantum memory schemes and the realization of light-matter interfaces [28–35]. In the protocol discussed here, two atomic ensembles are entangled by virtue of a dissipative mechanism which is induced by the application of a strong driving field. The generated entanglement can be accessed at any moment during an extended period of time, which makes it particularly useful for protocols, where it is not known in advance when the entangled state is needed (for example if probabilistic sub-routines are involved). If the entangled state is to be used, the driving field inducing the entangling mechanism is switched off before the actual protocol is run. Since entanglement is created between two ensembles, the resulting atomic state can either be used directly or be read out on demand using light-matter interface schemes [36, 37]. Another very interesting application is the use in continuous protocols, for example in dissipative quantum repeater schemes [38]. This type of scheme requires continuous entanglement for establishing high-quality steady state entanglement over large distances.

The remainder of the article is organized as follows. In Sec. II, we summarize the main results and explain the key features of the scheme. Sec. III is concerned with the

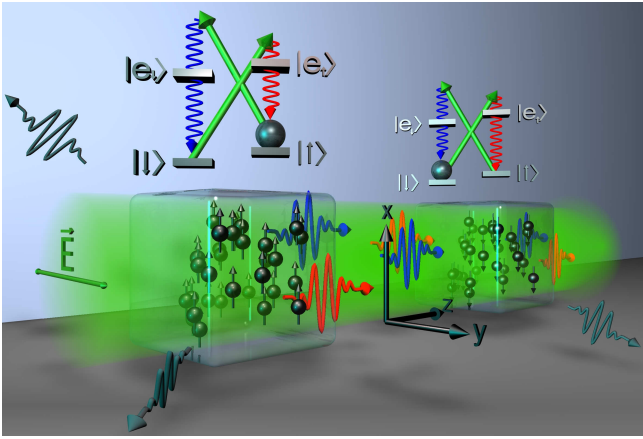


FIG. 1: Setup for dissipative entanglement generation between two spatially separated atomic ensembles. A homogeneous magnetic field, which is applied along the \hat{x} -direction defines the quantization axis and leads to a Zeeman splitting of the atomic ground states $|\uparrow\rangle$ and $|\downarrow\rangle$. A strong \hat{y} -polarized laser beam (shown in green) couples these states off-resonantly to the excited states $|e_\uparrow\rangle$ and $|e_\downarrow\rangle$ and to the light field in \hat{x} -direction (shown as wavy lines). The Zeeman shift Ω of the ground states leads to the emission of photons into two sideband modes centered around $\omega_L \pm \Omega$, where ω_L is the frequency of the applied laser field. The vacuum modes in \hat{x} -direction provide a common environment for the two atomic systems. Due to collective effects, the scattering of photons in this direction is enhanced.

creation of purely dissipative entanglement. We offer an intuitive explanation and data supporting this interpretation. We also compare the basic working mechanism to standard approaches and highlight the distinguishing features to the dissipative scheme discussed here. Thereafter, a hybrid method is described, where the dissipative mechanism is combined with continuous measurements on the light field. In Sec. IV, we explain how monitoring of the scattered photons can lead to an improvement of the produced entanglement in the presence of noise. In Sec. V, we present additional experimental material and Sec. VI concludes the paper.

II. OVERVIEW AND CENTRAL RESULTS

In this section, we provide a brief overview to the method of dissipative entanglement generation put forward in [1, 2] and [3]. We explain the main idea, introduce the experimental setup and summarize our main results.

Key idea

As outlined in the introduction, the entangling mechanism employed here is invoked by reservoir engineering and drives the system into a unique inseparable steady state. In the absence of other decoherence mechanisms, the steady state of the system (corresponding to the re-

duced density matrix after tracing out the environment) can be a pure state. In our case, the reservoir consists of a continuum of electromagnetic vacuum modes, which provide a common environment for the two ensembles. The atomic system can be coupled to this environment in a controlled fashion by applying suitable laser fields. More specifically, we consider the setup shown in Fig. 1. Each atomic ensemble consists of a large number N of hydrogen-like atoms with an internal level structure with two ground states $|\uparrow\rangle$ and $|\downarrow\rangle$. Both ensembles are driven by a far off-resonant \hat{y} -polarized coherent field. This strong classical driving field induces effective ground state transitions $|\uparrow\rangle \rightarrow |e_\uparrow\rangle \rightarrow |\downarrow\rangle$ and $|\downarrow\rangle \rightarrow |e_\downarrow\rangle \rightarrow |\uparrow\rangle$, which involve the emission of \hat{x} -polarized photons (compare Fig. 1). This way, the classical driving field couples the atomic system to the bath of electromagnetic modes in \hat{x} -polarization. The basic entangling mechanism can be understood by considering the \hat{x} -polarized vacuum modes in the direction of the laser field with wave-vector \mathbf{k}_L and the rest of the modes separately. The latter give rise to the standard spontaneous emission and represent noise processes. The former are shared by both ensembles and provide therefore the desired common environment. In the setting considered here, emission into the forward direction is collectively enhanced for a large optical depth d [33]. Hence, these modes can successfully compete with all the others and the entangling processes happen on a faster time scale than the undesired ones.

In our case, the target state is a two mode squeezed state which is entangled in the collective spin states of the two atomic ensembles $|\Psi_{\text{EPR}}\rangle$. This state is reminiscent of the entangled quantum state introduced by Einstein, Podolski and Rosen (EPR) [39]. $|\Psi_{\text{EPR}}\rangle$ is the simultaneous eigenstate with eigenvalue zero of two nonlocal operators A and B , $A|\Psi_{\text{EPR}}\rangle = 0$, $B|\Psi_{\text{EPR}}\rangle = 0$, where

$$A = \mu J_{\text{I}}^- - \nu J_{\text{II}}^-, \quad B = \mu J_{\text{II}}^+ - \nu J_{\text{I}}^+. \quad (1)$$

$J_{\text{I/II}}^\pm$ are collective spin operators with $J^- = \sum_i |\uparrow\rangle_i \langle \downarrow|$. $\mu = \cosh(r)$ and $\nu = \sinh(r)$, where r is the so-called squeezing parameter [40]. This type of entangled state is the main working horse for applications in quantum information science with atomic ensembles and continuous variable systems in general [41]. Entanglement can be verified and quantified by the parameter $\xi = \Sigma_J / (2|\langle J_x \rangle|) = (\mu - \nu)^2$, with $\Sigma_J = \text{var}(J_{y,\text{I}} - J_{y,\text{II}}) + \text{var}(J_{z,\text{I}} - J_{z,\text{II}})$. $\xi < 1$ certifies the creation of an inseparable state [42, 43].

The existence of a steady state $|\Psi_{\text{EPR}}\rangle$ with $A|\Psi_{\text{EPR}}\rangle = B|\Psi_{\text{EPR}}\rangle = 0$ can be understood as an interference process where a (\hat{x} -polarized) photon, which is emitted in forward direction with a given frequency could have been originated from either of the two ensembles. For a particular atomic state, $|\Psi_{\text{EPR}}\rangle$, these two process interfere destructively, such that no photon is scattered into this direction. As a consequence, the interaction with the

laser is switched off and the state remains the same. This interpretation can be quantitatively understood in terms of a master equation.

In the scheme reported on here, the system-reservoir coupling is engineered such that it gives rise to a dissipative dynamics which is governed by

$$\frac{d}{dt}\rho = \mathcal{L}_{\text{ent}}(\rho) \quad (2)$$

$$\propto (A\rho A^\dagger - A^\dagger A\rho + \text{H.C.}) + (B\rho B^\dagger - B^\dagger B\rho + \text{H.C.}).$$

It can be shown [3] that $\rho_{\text{EPR}} = |\Psi_{\text{EPR}}\rangle\langle\Psi_{\text{EPR}}|$ is the unique steady state of this evolution. In order to obtain a two mode squeezed state, the system is coupled to two reservoirs, which give rise to the jump operators A and B respectively. To this end, the ensembles are placed in a homogeneous magnetic field which causes a Zeeman splitting of the atomic ground states Ω . Due to the different ground state energies, photons are scattered into two different frequency bands centered around $\omega_L \pm \Omega$, which we will refer to as upper (blue) and lower (red) sideband respectively. For a sufficiently large separation in frequency space ($\Omega \gg \Gamma_{\text{Atomic}}$, where Γ_{Atomic} is the largest effective atomic transition rate for ground state transitions $|\uparrow\rangle \leftrightarrow |\downarrow\rangle$ [3]), the continua of modes in the lower and upper sideband can be treated as independent reservoirs (compare A). The first (second) term in Eq. (2) is due to the interaction with the photons in the lower (upper) sideband. Note that the jump operators defined in Eq. (1) are nonlocal (i.e. involve atomic operators referring to both, the first and the second ensemble) and can give therefore rise to an entangled steady state. As explained above, it originates from the interference between processes where a photon is emitted in forward direction by the first or the second ensemble. Other processes can be included in the form of additional terms in the master equation $\frac{d}{dt}\rho = \mathcal{L}_{\text{ent}}(\rho) + \mathcal{L}_{\text{noise}}(\rho)$, where $\mathcal{L}_{\text{noise}}(\rho)$, summarizes undesired processes such as spontaneous emission, collisions and fluctuating magnetic fields. A key point lies in the fact that the rate of the entangling processes ($\mathcal{L}_{\text{ent}}(\rho)$) scales with the optical thickness (due to collective effects which originate from constructive interference involving each individual atom within a single ensemble), whereas the rate of the detrimental processes does not. Thus, for sufficiently optically thick samples, the creation of entanglement in a steady state is possible even in the presence of noise (see Eq. (B1) in B).

Setup and experimental results

The experiment is carried out using ^{133}Cs vapor at room temperature. The two-level subsystem is encoded in the two outermost hyperfine levels of the $6S_{1/2}$ ground state within the manifold with total spin $F = 4$ [44]. We identify $|\uparrow\rangle_I \equiv |F = 4, m_F = 4\rangle$, $|\downarrow\rangle_I \equiv |F = 4, m_F = 3\rangle$ and $|\uparrow\rangle_{II} \equiv |F = 4, m_F = -3\rangle$, $|\downarrow\rangle_{II} \equiv |F = 4, m_F = -4\rangle$ (where m_F is the magnetic quantum number). The atoms are confined in cubic glass cells which are separated by a distance of approximately 0.5m and have a

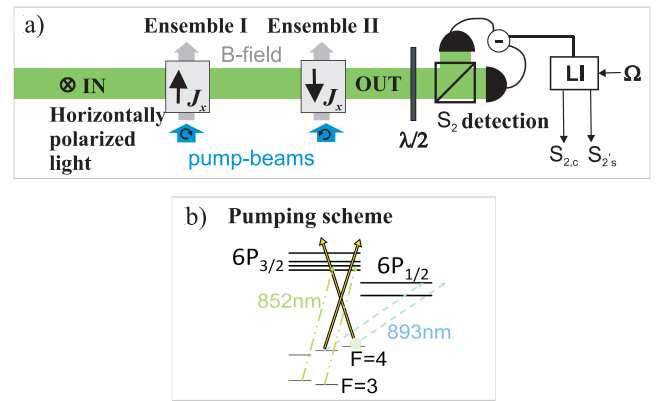


FIG. 2: a) Experimental setup. The horizontally polarized probe light shown in green passes through two oppositely oriented atomic ensembles. The orientation is generated via optical pumping. The optical pumping beams are depicted in blue. Behind the two atomic cells, the S_2 detector signal is processed by the lock-in amplifier (LA) to take measurements on the atomic quantum spin components $J_{y,z}$ in the rotating frame. b) shows the optical pumping scheme. The relevant laser frequencies and polarizations are indicated in a level scheme.

spatial extent of 2.2cm. Each cell contains 10^{12} atoms and is equipped with a paraffin-based spin-preserving coating. The experimental setup is sketched in Fig. 2a. The two ensembles are prepared in oppositely oriented coherent spin states (CSS). This is achieved by optically pumping the atoms of the ensembles into $m_F = \pm 4$ in the \hat{x} -direction respectively. The circularly polarized pump lasers are depicted in blue and Fig. 2b shows the atomic level structure, indicating laser frequencies and polarization. The strong probe beam which is initially polarized in \hat{y} -direction transverses the atoms in the \hat{z} -direction. Behind the cells, the detection system is set up.

In [1], two types of results have been obtained. Firstly, entanglement has been created purely dissipatively, demonstrating that this type of processes can be harnessed for tasks in Quantum Information Science. In this series of experiments, entanglement has been maintained for a time span, which is an order of magnitude longer than the time intervals for which entanglement could be sustained in this system so far [33]. Entanglement has been obtained in a quasi steady state rather than in a true steady state due to the multi-level structure of Cesium. As opposed to the two-level model discussed above, atoms can leave the two-level system by undergoing transitions to other internal states. The entangling processes are fast compared to these undesired transitions. The desired dynamics with respect to the two-level subsystem reaches a steady state, but since it is superposed by the slow detrimental processes involving atom losses, entanglement disappears.

In a second series of experiments, strong pump and re-pump fields have been applied in order to transfer the

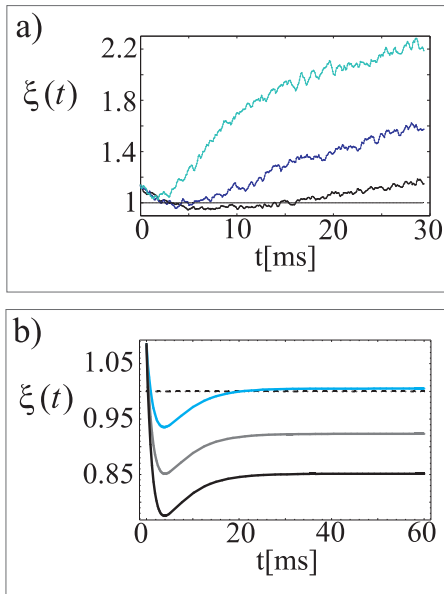


FIG. 3: Entanglement generated by dissipation a) Entanglement for different detunings $\delta\Omega$ of the magnetic fields. The different curves correspond to $\delta\Omega = 0$ (black), $\delta\Omega = 20\text{Hz}$ (violet) and $\delta\Omega = 40\text{Hz}$ (blue). b) Dissipatively generated steady state entanglement. Predicted time evolution of $\xi(t)$ in the presence of strong pump and repump fields for $d = 55$, (blue), $d = 100$ (grey) and $d = 150$ (black). The other parameters take values close to the ones used in [1], as explained in C.

atoms back, which left the two-level system. These incoherent fields lead to increased noise contributions, which prevents the generation of a purely dissipative steady state in this particular setting. However, by combining the dissipative mechanism with continuous measurements on the light field, a true steady state has been obtained. In the following, we consider the generation of entanglement by dissipation in more detail.

III. PURELY DISSIPATIVE ENTANGLEMENT

This section is concerned with the purely dissipative generation of entanglement. The basic mechanism is explained and further substantiated by additional experimental data. Moreover, the perspectives for obtaining steady state entanglement for multi-level systems is discussed.

Entanglement creation by virtue of interference

As mentioned earlier, the underlying mechanism can be understood as an interference effect in the dissipative channel. Due to destructive interference, no photon is scattered into the forward direction in the steady state. Accordingly, no measurement needs to be performed on the light field. Additional evidence that the entanglement is produced by the collective dissipation process is

provided by its dependence on the dephasing between spin coherences of the two ensembles. To demonstrate this dependence, we introduce a detuning $\delta\Omega = \Omega_I - \Omega_{II}$ of the Larmor frequencies of the two ensembles by tuning the bias magnetic fields. Fig. 3a shows that already at $\delta\Omega = 20\text{Hz}$ entanglement disappears. This can be understood as a consequence of the "which way" information (or "which ensemble" information in this case) provided by the distinguishability of the photons scattered from the two ensembles into the sideband modes $\omega_L \pm \Omega_I$ and $\omega_L \pm \Omega_{II}$. Hence the atomic samples do not share the same reservoir any more and entanglement disappears. Note that the effect demonstrated in the experiment can not be understood in terms of photons which are spontaneously emitted by the first ensemble interacting with the second one. Due to the large detuning ($\Delta = 850\text{MHz}$), the interaction of a single photons emitted by the first ensemble with atoms in the second one is negligible in the parameter regime accessible in the experiment. Here, atomic transitions are to a very good approximation only induced by the classical driving field (accordingly, the input-output relations for atoms in the second sample are identical with those in the absence of the first ensemble).

Comparison of dissipative entanglement generation with other methods

There exists a large variety of methods for creating entanglement between two quantum systems. In particular, several methods have been devised and demonstrated for entangling atomic ensembles. Even though some schemes, which have been experimentally implemented share similarities with the one described here, they are fundamentally different. In the following, we explain this in detail and highlight the features of the method realized here in comparison with previously demonstrated ones.

In standard approaches, which are based on a coherent interaction followed by a measurement [28, 33, 43, 45–53], two atomic ensembles A, and B are prepared in specific pure states $|a\rangle_A$, and $|b\rangle_B$. An additional system, E, which typically corresponds to certain modes of the electromagnetic field, is also initialized in a specific state, for example the vacuum $|0\rangle_E$. For appropriately chosen external parameters such as the frequency and polarization of applied laser fields, the interaction of system E with A and B gives rise to an entangled state $|\Psi\rangle = U|a, b\rangle_{A,B}|0\rangle_E$. If system E is measured, e.g. using a beam splitter and single-photon detectors, or by means of homodyne detection, the state of systems A and B is projected onto an entangled state, $|\Phi(e)\rangle_{A,B}$. This state depends on the outcome of the measurement, e . If no measurement is performed (which corresponds to averaging with respect to the possible measurement outcomes [54]) the resulting state is not entangled. For instance, the DLCZ protocol [45], yields a separable state if the photons emitted by the ensembles are not detected.

Dissipative methods can be described as follows. $|a\rangle_A$, $|b\rangle_B$, and $|0\rangle_E$ denote again the initial states of systems A, B and E respectively. Due to the interaction of system E with A and B, the state $|\Psi(t)\rangle = U(t)|a, b\rangle_{A,B}|0\rangle_E$ is created, where the dependence of the resulting quantum state on the time t is explicitly indicated. Under ideal conditions, i.e. if systems A and B do not couple to other environments, the interaction of A and B with E can be engineered such that the atomic system evolves towards an entangled state. In contrast to the schemes described above, the implementation of this entangling dynamics does not require measurements on system E. This type of behavior can occur if system E possesses an infinite number of degrees of freedom, such that a non-unitary dynamics drives the system towards a fixed state. Due to this property, E is typically referred to as environment and the corresponding interaction with systems A and B is referred to as dissipative process. Dissipative phenomena of this kind are best described by means of master equations. To this end, the environment is traced out and an equation for the reduced density operator of systems A and B, ρ , is derived as described in A. In the presence of other environments, the dissipation induced by the coupling of A and B to system E can still create entanglement with a life time, which exceeds the decoherence times due to these extra noise sources significantly, if the corresponding (uncontrolled) coupling is sufficiently weak. Note further, that typically, noise processes can be included in the master equation description as it is done in the present work.

In the experiment discussed here, entanglement induced by dissipation has been observed. In particular, in contrast to approaches which have been previously implemented, entanglement is obtained without using measurements on the quantum state of the environment [55]. Furthermore, systems A and B remain entangled for 40ms. This entanglement life-time is at least by a factor 16 longer than the decoherence time induced by other noise sources. It has been experimentally verified that in the absence of the dissipative process, the measured entanglement life time is limited to 2.5ms due to the remaining noise sources such as collisions or inhomogeneities of the applied magnetic fields.

Dissipative methods exhibit another distinctive feature, which is present for an ideal two-level system (compare [3]), but not in the multilevel description of the experiment. For long times $t \rightarrow \infty$, systems A and B decouple from the environment E, $|\Psi(t)\rangle \rightarrow |\Phi\rangle_{A,B}|E(a, b, t)\rangle_E$ under ideal conditions, i.e. in the absence of additional noise sources. Remarkably, the desired state $|\Phi\rangle_{A,B}$ is reached irrespective of the initial state of systems A and B which can be highly mixed. Moreover, except for an initial waiting time, no special timing is required. This behavior is again due to the fact that E possesses an infinite number of degrees of freedom, which guarantees that revival effects are not present. This way, entropy is

transferred from the system to the environment, which drives A and B into a particular steady state, which depends only on the engineered coupling.

Using dissipative methods, a mixed but still entangled steady state can be reached even in the presence of additional noise sources, as long as the coupling of A and B to other environments is sufficiently weak compared to the engineered dissipative processes. This opens up the possibility to keep systems A and B entangled for arbitrarily long times.

Perspectives for creating purely dissipative steady state entanglement in multi-level systems.

Below, we investigate the possibility of generating purely dissipative steady state entanglement in atoms with multi-level ground states. The main reason, why the system in the experiment reported on in [1] does not display purely dissipatively generated entanglement in a steady state is the depopulation of the relevant two-level subsystem due to spontaneous emission which transfers the atoms into other Zeeman levels. The depopulation of the relevant levels can be avoided by applying strong laser fields, which transfer atoms back. However, these fields introduce additional decoherence processes which inhibit the creation of entanglement in a steady state. This problem can be circumvented by increasing the optical depth of the atomic ensembles such that the entangling dissipative process prevails over the noise processes and dominates the dynamics.

We consider this scenario by including additional σ_{\pm} polarized pump and repump fields, which induce resonant transitions with $\Delta m_F \pm 1$ in the first/second ensemble in the model. Pump fields drive transitions within the manifold of atomic states with $F = 4$ and repump fields transfer atoms from states with $F = 3$ back to $F = 4$. As explained in C, we estimate the effect of these fields using a simplified model, which has been used in [1] to fit the experimental data. Fig. 3b shows the predicted time evolution of entanglement for $d = 55; 100; 150$ in the presence of both, pump and repump fields (in [1], an optical depth of $d = 55$ was used). The other parameters used in this calculation take values close to the ones used in [1]. The theory predicts that under the present maximal optical depth $d = 55$, the steady state atomic variance is just slightly above the separability criterion (this has also been confirmed experimentally). However, the experimental realization of purely dissipative steady state entanglement should be feasible along two possible routes. Firstly, atoms possessing two-level electronic ground states can be used, for example Ytterbium (^{171}Yb) [56, 57]. In this case, the two-level theory formulated here can be directly implemented, avoiding additional dynamics which leads to the growth of ξ with time. Alternatively, a true dissipatively generated steady state using multi-level ground states can be achieved for higher optical depths, which can be obtained, for example, by placing the atoms inside a low finesse optical cavity.

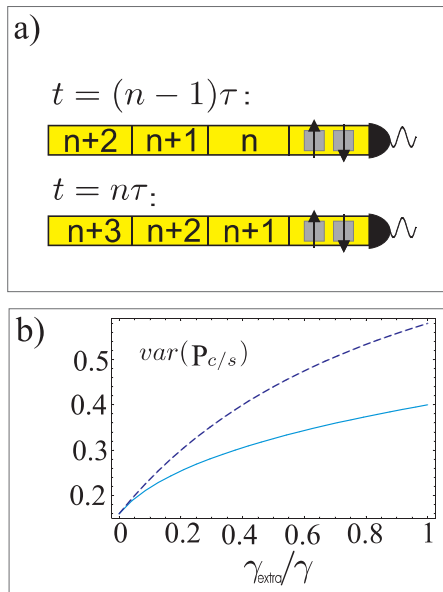


FIG. 4: **Steady state entanglement assisted by measurements.** a) Illustration of the interaction of atoms and light in terms of spatially localized modes b) Squeezed atomic variance $\text{var}(P_{c/s})$ in the steady state versus the ratio $\gamma_{\text{extra}}/\gamma_s$ in the absence of measurements (dashed line) and if the y -quadrature of the scattered light field is measured (full line). γ_{extra} and γ_s denote the rates of the desired entangling processes and the atomic decay respectively.

In [1], we devised and implemented an alternative approach, which enables the creation of entanglement which persists for arbitrarily long times. This alternative approach combines the dissipative mechanism with continuous measurements as explained below.

IV. DISSIPATIVE ENTANGLEMENT ASSISTED BY MEASUREMENTS

In the following, we show by means of a simple model how measurements on the light field can improve the generation of entanglement under the dissipative dynamics described above in the presence of noise sources. In the basic model employed here to illustrate the relevant effects, the Holstein-Primakoff approximation [58] is used to describe the atomic system and noise is included in the form of decay of the transverse spin components J_y and J_z at a rate γ_{extra} (a more detailed discussion is to be published elsewhere). In this subsection, the dissipative generation of entanglement assisted by measurements is explained in terms of input-output relations, since this approach is more illustrative than the master equation formalism employed in Sec. II. Both descriptions are equivalent and yield the same results.

For large, strongly polarized atomic ensembles, collective spins can be described by bosonic modes in terms

of the quadratures

$$X_{I/II} = J_{y,I/II}/\sqrt{|\langle J_{x,I/II} \rangle|},$$

$$P_{I/II} = \pm J_{z,I/II}/\sqrt{|\langle J_{x,I/II} \rangle|}.$$

Light propagates in \hat{z} -direction (see Fig. 1) and interacts with the atomic ensembles. We consider here a one-dimensional model which includes only light scattered in forward direction. Processes corresponding to scattering of photons into other directions enter in the form of noise. Light is characterized in terms of spatially localized modes [59, 60]

$$y(z) = \frac{1}{\sqrt{4\pi}} \int_b d\omega \left(a_\omega e^{\frac{i}{c}(\omega - \omega_L)z} + H.C. \right),$$

$$q(z) = \frac{-i}{\sqrt{4\pi}} \int_b d\omega \left(a_\omega e^{\frac{i}{c}(\omega - \omega_L)z} - H.C. \right),$$

where c is the speed of light. b and ω_L are the bandwidth and central frequency of the applied laser field. The operators for spatially localized field modes $y(z)$ and $q(z)$ obey the canonical commutation relation $[y(z), q(z')] = ic\delta_b(z - z')$, where the deltafunction has a width of the order c/b . The spatial argument z refers to the distance along the propagation direction \hat{z} . Atoms and light interact according to $H = H_A + H_L + H_{\text{int}}$, where $H_A = \frac{\Omega}{2} (X_I^2 + P_I^2) - \frac{\Omega}{2} (X_{II}^2 + P_{II}^2)$ describes the Zeeman splitting of the atomic ground states. Due to the applied magnetic field, the transverse components of the collective spin described by $X_{I/II}$ and $P_{I/II}$ precess at the Larmor frequency Ω . H_L represents the free propagation of light $\frac{d}{dt}y(z) = i[H_L, y(z)] \cong -c\frac{d}{dz}y(z)$. The interaction of the light field with two pointlike atomic ensembles [61] located at $z = 0$ and $z = R$ is given by

$$H_{\text{int}} = \sqrt{2\gamma_s} \left(\frac{1}{Z} X_I y(0) + Z P_I q(0) \right)$$

$$+ \sqrt{2\gamma_s} \left(\frac{1}{Z} X_{II} y(R) + Z P_{II} q(R) \right),$$

where $Z = \mu + \nu$ and $1/Z = \mu - \nu$. We assume in the following, that the distance R between the ensembles can be neglected, which is justified for $\Gamma_{\text{Atomic}}R \ll c$, where Γ_{Atomic} is the effective rate at which transitions between ground states occur, and $L^2k_L \gg R$, where L is the spatial extend of an atomic ensemble and k_L is the wave vector of the driving field. The former is a necessary condition to neglect retardation effects, while the latter is used in the calculation of averaged emission rates for fast moving atoms (compare A and [3]). Both conditions are well fulfilled for the parameter regime of the experiment, where the effective decay rates are of the order of few ms and R is on the order of a meter (L is about 2cm and k_L on the order of 10^7m^{-1}). The resulting Heisenberg equations can be solved by changing to a coordinate system rotating at the Larmor frequency

Ω and performing the variable transformation $\zeta = ct - z$ such that $\bar{y}(\zeta, t) = y(ct - z, t)$. We introduce exponential $\cos(\Omega t)$ and $\sin(\Omega t)$ modulated light functions

$$\begin{aligned} y_{c,\pm}^{\text{in}} &= \frac{1}{\mathcal{N}_{\pm}} \int_0^T e^{\pm\gamma_s t} \cos(\Omega t) \bar{y}(\zeta, 0), \\ q_{c,\pm}^{\text{in}} &= \frac{1}{\mathcal{N}_{\pm}} \int_0^T e^{\pm\gamma_s t} \cos(\Omega t) \bar{q}(\zeta, 0), \end{aligned} \quad (3)$$

with $\mathcal{N}_+ = \frac{2\sqrt{\gamma_s}}{\sqrt{e^{2\gamma_s T} - 1}}$ and $\mathcal{N}_- = \frac{2\sqrt{\gamma_s}}{\sqrt{1 - e^{-2\gamma_s T}}}$. $y_{s,\pm}^{\text{in}}$ and $q_{s,\pm}^{\text{in}}$ are defined analogously. We assume that the Larmor precession is fast compared to the atomic evolution ($\Omega T \gg 1$), such that the operators describing the sin and cos modulated light modes are canonical and independent, $[y_{c,\pm}, q_{c,\pm}] = [y_{s,\pm}, q_{s,\pm}] = i$ and $[y_{c,\pm}, q_{s,\pm}] = [y_{s,\pm}, q_{c,\pm}] = 0$. This yields

$$\begin{aligned} X_{c/s}^{\text{out}} &= e^{-\gamma_s T} X_{c/s}^{\text{in}} + Z \sqrt{1 - e^{-2\gamma_s T}} q_{c/s,+}^{\text{in}}, \\ P_{c/s}^{\text{out}} &= e^{-\gamma_s T} P_{c/s}^{\text{in}} - \frac{1}{Z} \sqrt{1 - e^{-2\gamma_s T}} y_{c/s,+}^{\text{in}}, \\ y_{c/s,-}^{\text{out}} &= e^{-\gamma_s T} y_{c/s,+}^{\text{in}} + Z \sqrt{1 - e^{-2\gamma_s T}} P_{c/s}^{\text{in}}, \\ q_{c/s,-}^{\text{out}} &= e^{-\gamma_s T} q_{c/s,+}^{\text{in}} - \frac{1}{Z} \sqrt{1 - e^{-2\gamma_s T}} X_{c/s}^{\text{in}}, \end{aligned} \quad (4)$$

where $X_c = \frac{1}{\sqrt{2}}(X_I + X_{II})$, $P_c = \frac{1}{\sqrt{2}}(P_I + P_{II})$ and $X_s = \frac{-1}{\sqrt{2}}(P_I - P_{II})$, $P_s = \frac{1}{\sqrt{2}}(X_I - X_{II})$ was used. As a next step, we include continuous measurements on the light field and consider the corresponding time evolution of the atomic state in the Schrödinger picture. The continuous interaction and measurement process shown in Fig. 1 is illustrated schematically in Fig. 4a in a discretized way. Spatially localized light modes correspond here to infinitesimally short pulses of duration $\tau \sim 1/b$ (where b is the bandwidth of the incident laser field as explained above), which interact successively with the atomic system. Each of these spatially localized light modes is initially in the vacuum state, such that the quantum state at time $t = n\tau$ is given by $|\Psi(t)\rangle_A |0\rangle_{L,n+1}$, where $|\Psi(t)\rangle_A$ denotes the atomic state at time t . Then atoms and light are subject to an entangling interaction resulting in the quantum state $e^{-iH\tau} |\Psi(t)\rangle_A |0\rangle_{L,n+1}$. Finally, the y -quadrature of the light field is measured, yielding the measurement outcome y_n such that $|\Psi(t + \tau)\rangle_A = \frac{1}{\sqrt{P(y_n)}} \int_{L,n+1} \langle y_n | e^{-iH\tau} |0\rangle_{L,n+1} |\Psi(t)\rangle_A$, where $P(y_n)$ is the probability to obtain the result y_n . The resulting expression can be expanded up to first order in the parameter τ yielding a differential equation for the time evolution of the atomic system. The atomic state obtained after the measurement depends on the measurement outcome y_n . We consider here Gaussian quantum states, i.e. states with a Gaussian Wigner function. These states are fully characterized by their first and second moments, - prominent examples include coherent as well as two mode squeezed states. The Gaussian character of a state is preserved under the evolution of Hamiltonians, which are at most quadratic in

the system operators and under Gaussian measurements such as homodyne detection. Since we consider all interactions and measurements to be of this kind and all states to be Gaussian, the entanglement of the resulting state is completely determined by the atomic variance $\text{var}(P_{c/s})$, which does not depend on y_n [62]. Therefore the resulting entanglement is independent of the measurement outcome. If the measurement results are traced out ($\rho(t+\tau) = \sum_{y_n} M_n \rho(t) M_n^\dagger$, where $M_n = \langle y_n | e^{-iH\tau} |0\rangle_{L,n+1}$), and the resulting expression is evaluated to first order in τ , the master equation used in Sec. II and A is recovered, if the spin operators are replaced by creation and annihilation operators within the Holstein-Primakoff approximation [58]. The whole process can be conveniently described by means of the Gaussian formalism, where atomic states are expressed in terms of their covariance matrix Γ_c , and displacement vector \mathbf{D} , which display the second moments (variances and covariances) and first moments (mean values) of the system respectively. In particular, this formalism allows one to easily calculate the variances of atomic quadratures after the Gaussian measurement of the y -quadrature of the light field, $\text{var}(P_{c/s})_{\text{cond}}$ at the end of each time step depending on the variance prior to the measurement

$$\text{var}(P_{c/s})_{\text{cond}} = \text{var}(P_{c/s}) - \frac{\langle P_{c/s} y_{c/s} + y_{c/s} P_{c/s} \rangle^2}{4\text{var}(y_{c/s})}, \quad (5)$$

where $y_{c/s}$ and $q_{c/s}$ refer here to the localized light mode interacting with the ensemble in the n^{th} time step and $\gamma_s \tau \ll 1$ is assumed. This way, a differential equation for the squeezed atomic variances is derived. In the ideal case,

$$\text{var}(P_{c/s})_{\text{cond}}(t+\tau) = \text{var}(P_{c/s})_{\text{cond}}(t) + \text{var}(P_{c/s})_{\text{cond}}(t) (1 - \text{var}(P_{c/s})(t) Z^2) \gamma_s \tau,$$

which yields

$$\text{var}(P_{c/s})_{\text{cond}}(t) = \frac{1}{e^{-\gamma_s t} (\text{var}(P_{c/s})(0))^{-1} + Z^2 (1 - e^{-\gamma_s t})},$$

whereas in the absence of measurements,

$$\text{var}(P_{c/s})(t) = e^{-\gamma_s t} \text{var}(P_{c/s})(0) + \frac{1}{Z^2} (1 - e^{-\gamma_s t}).$$

Both time evolutions result in a steady state with $\text{var}(P_{c/s})_{\infty} = 1/Z^2 = (\mu - \nu)^2$, since atoms and light decouple for $t \rightarrow \infty$. Accordingly, the steady state entanglement can not be improved by means of measurements on the light field in the ideal case. The situation is different in the presence of noise sources, which prevent the decoupling of atoms and light. In this case, residual atom-light correlations persist in the steady state and measurements on the light field can be used to improve the entanglement. Here, we illustrate this effect by including atomic transverse decay at a rate γ_{extra} [63]. If

the y -quadrature of the scattered light field is measured, one obtains

$$\xi_{\text{cond},\infty} = \frac{1}{2Z^2} \left(1 - \frac{\gamma_{\text{extra}}}{\gamma_s} + \sqrt{\left(1 - \frac{\gamma_{\text{extra}}}{\gamma_s}\right)^2 + 4Z^2 \frac{\gamma_{\text{extra}}}{\gamma_s}} \right).$$

Fig. 4b shows that for $\gamma_{\text{extra}} > 0$, the steady state entanglement described by this equation is higher than the steady state if no measurements are performed, which is given by

$$\xi_{\infty} = \frac{\frac{1}{Z^2} \gamma_s + \gamma_{\text{extra}}}{\gamma_s + \gamma_{\text{extra}}}.$$

Note that in principle, all measurement results $y(t)$ obtained during the continuous measurement procedure could be used to perform feedback operations which stabilize the atomic state at a certain position in phase space. However, this is not necessary here, since the atomic quantum state at time t depends only on the recent history of the measurements, i.e. on $y(t')$ for $t_{ss} \leq t' \leq t$, where t_{ss} is the time it takes to reach the steady state. For the dissipative processes considered here, the atomic state $\rho(t)$ is memoryless regarding events which occurred in a time interval longer than t_{ss} . Thus, only measurement results obtained during a fixed time interval t_{ss} , which is independent of t are needed to localize the atomic state in phase space.

V. EXPERIMENTAL ATOMIC STATE RECONSTRUCTION

The experimental setup is depicted in Fig. 2 and described in the caption and the surrounding text. This section is focussed on the characterization of the atomic state via measurements on light which has interacted with the atomic ensembles.

The light observable of interest is the Stokes operator S_2 given by the difference of the number of photons polarized in $\pm 45^\circ$. In the specific setting discussed here, the probe beam is strongly polarized in \hat{y} -direction and the \hat{x} -polarization represents the polarization mode of interest for measurement as discussed in Sec. IV. Then the Stokes operator $S_2 \approx \sqrt{\phi/2} \cdot y$, where ϕ is the photon flux. S_2 can be measured with polarization homodyning techniques as depicted in Fig. 2. The light beam is sent through a halfwave plate and a polarizing beam splitter (PBS). The signals from the detectors situated in the output ports of the PBS are subtracted and the difference signal is analyzed at the Larmor frequency Ω with a lock-in amplifier, since we are interested in detecting a signal from the spins in the rotating frame. Additionally the measurement outcome can be weighted with suitable mode functions $f(t)$ and after suitable normalization we are thus able to measure the light observables $y_{c,s-}$ or $y_{c,s+}$ defined in Eq. (3).

A. Atomic state reconstruction

Now, the variances of the collective atomic operators $P_c^{\text{in}} = 1/\sqrt{2}(P_I^{\text{in}} + P_{II}^{\text{in}})$ and $P_s^{\text{in}} = 1/\sqrt{2}(X_I^{\text{in}} - X_{II}^{\text{in}})$ can be found from measurements on the transmitted light. From the variances of the outgoing operators $y_{c,s-}$, using the input-output relations given in Eq. (4), it follows:

$$\begin{aligned} \text{var}(P_c^{\text{in}}) &= \frac{1}{\kappa^2} (\text{var}(y_{c-}^{\text{out}}) - \sigma_{in}^2 (1 - \frac{\kappa^2}{Z^2})), \\ \text{var}(P_s^{\text{in}}) &= \frac{1}{\kappa^2} (\text{var}(y_{s-}^{\text{out}}) - \sigma_{in}^2 (1 - \frac{\kappa^2}{Z^2})), \end{aligned} \quad (6)$$

where σ_{in}^2 is the shot noise of light, assuming that the incoming light is in a coherent state. The coupling constant is defined as $\kappa = Z\sqrt{1 - e^{-2\gamma_s T}}$. The normalized EPR variance of atomic noise is $\xi = \text{var}(P_c^{\text{in}}) + \text{var}(P_s^{\text{in}}) = \text{var}(P_I^{\text{in}} + P_{II}^{\text{in}})/2 + \text{var}(X_I^{\text{in}} - X_{II}^{\text{in}})/2$.

B. Including decay and detection efficiency

To include the decay of the atomic spin due to spontaneous emission, magnetic field instabilities, etc. into the input-output equations (Eq. 4), we assume a decay with the rate γ_{extra} towards the CSS. Since the interaction times which are used to perform the read out are short, this is an adequate approximation. The atomic part of the input-output equations becomes

$$\begin{aligned} P_{c,s}^{\text{out}} &= P_{c,s}^{\text{in}} \cdot e^{-\gamma T} - \frac{\kappa}{Z^2} y_{c,s+}^{\text{in}} + \epsilon \sqrt{1 - e^{-2\gamma T}} \cdot F_{p,c/s,+}, \\ X_{c,s}^{\text{out}} &= X_{c,s}^{\text{in}} \cdot e^{-\gamma T} + \kappa q_{c,s+}^{\text{in}} + \epsilon \sqrt{1 - e^{-2\gamma T}} \cdot F_{x,c/s,+}, \end{aligned} \quad (7)$$

with the two-cell noise operators $F_{i+} = 1/N_F \int_0^T e^{-\gamma(T-t)} F_i(t) dt$ and $\langle F_i^2 \rangle = \frac{1}{2}$ and $\epsilon^2 = \gamma_{\text{extra}}/\gamma$. The relevant light mode is exponentially growing with the total decay rate $\gamma = 1/T_2 = \gamma_s + \gamma_{\text{extra}}$. The coupling constant is reduced due to the decay and defined as: $\kappa = Z\sqrt{(1 - \epsilon^2)(1 - e^{-2\gamma T})}$.

Also the equations for the light are adjusted accordingly:

$$\begin{aligned} y_{c,s-}^{\text{out}} &= \epsilon^2 y_{c,s-}^{\text{in}} + y_{c,s+}^{\text{in}} \sqrt{1 - \kappa^2/Z^2} (1 - \epsilon^2) + \kappa \sqrt{1 - \epsilon^2} P_{c,s}^{\text{in}} \\ &\quad + \epsilon \sqrt{1 - \epsilon^2} Z (F_{p-} - \sqrt{1 - \kappa^2/Z^2} F_{p+}), \\ q_{c,s-}^{\text{out}} &= \epsilon^2 q_{c,s-}^{\text{in}} + q_{c,s+}^{\text{in}} \sqrt{1 - \kappa^2/Z^2} (1 - \epsilon^2) - \kappa/Z^2 \sqrt{1 - \epsilon^2} X_{c,s}^{\text{in}} \\ &\quad + \epsilon \sqrt{1 - \epsilon^2} Z (F_{x-} - \sqrt{1 - \kappa^2/Z^2} F_{x+}). \end{aligned} \quad (8)$$

The non orthogonal exponentially growing and falling light modes are now mixed due to the decay.

The reconstruction equation (Eq. 6) must then be adjusted accordingly:

$$\begin{aligned} \text{var}(P_c^{\text{in}}) &= \frac{1}{\kappa^2} (\text{var}(y_{c-}^{\text{out}}) - U^2 \cdot \sigma_{s,in}^2 - V^2 \langle F_i^2 \rangle), \\ \text{var}(X_s^{\text{in}}) &= \frac{1}{\kappa^2} (\text{var}(y_{s-}^{\text{out}}) - U^2 \cdot \sigma_{c,in}^2 - V^2 \langle F_i^2 \rangle), \end{aligned} \quad (9)$$

with the corrected, reduced coupling constant and $U^2(\kappa^2, T_2)$ and $V^2(\kappa^2, T_2)$ which can be calculated directly from Eq. (8) [64]. To extract the atomic noise from the light noise measurements, it is therefore only necessary to know the coupling constant κ , for which a measurement procedure is explained below and the decay time T_2 which can also easily be measured.

Additionally, the detection efficiency $\eta = 0.84(4)$ which arises from light losses and imperfect detection can be included by assuming a beam-splitter with transmission η .

C. Measurement of the coupling strength

The most important experimental parameter for the reconstruction is the coupling constant κ . It would be possible to determine κ^2 , by performing noise measurements on known atomic states, e.g. the CSS or the thermal atomic state. However, imperfect state preparation or additional noise sources can spoil such measurements. The approach we implement here is therefore based on measurements of mean values as opposed to noise measurement. The modus operandi is to transfer a coherent light state with a known displacement to the atoms and then read out the atomic state [34, 65].

First, a pulse is sent through two oppositely oriented atomic samples with a displacement in $q_{c,s}^{1st}$, so in S_z . Following Eq.4 and assuming that the atoms possess no initial displacement, this leaves the atomic sample with a mean value in the X -quadratures.

$$\langle X_{c,s}^{out} \rangle = \kappa \langle q_{c,s+}^{1st} \rangle. \quad (10)$$

To be able to read out those atomic mean values via a measurement on $y_{c,s}$ and thus gain information on κ , we apply a $\pi/2$ -pulse to the atomic spin rotating X into P . This can be done by adding a magnetic field in the \hat{x} -direction, so that the spins rotate a little faster or slower in between the pulses and $J_{z,I} \rightarrow J_{y,I}$ and $J_{y,II} \rightarrow J_{z,II}$, leading to $X_{c,s} \rightarrow P_{c,s}$. Then we send a second light pulse for the read out. The outcome of the light measurement of the second pulse reveals

$$\langle y_{c,s-}^{2nd} \rangle = \kappa \langle X_{c,s}^{out} \rangle = \kappa^2 \langle q_{c,s+}^{1st} \rangle. \quad (11)$$

The coupling strength can be calculated: $\kappa^2 = \frac{\langle y_{c,s-}^{2nd} \rangle}{\langle q_{c,s+}^{1st} \rangle}$.

The displaced coherent light states are produced with the help of an electro optical modulator (EOM) [66]. The strongly polarized beam is sent through an EOM whose optical axis is slightly tilted compared to the input polarization. Then a DC voltage and a small modulation at 322 kHz can be used to rotate a small portion of the large polarization component in \hat{y} -direction into the x -polarization mode. The value of the DC voltage determines the phase of the modulation in phase space, so the position in the S_2 - S_3 plane. The strength and phase of the RF modulation determine the size of the displacement of the cosine and sine modes.

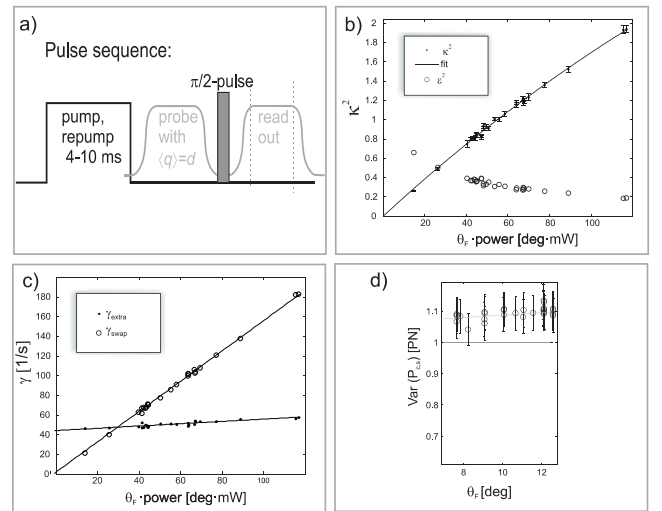


FIG. 5: In a) the pulse sequence is shown. The probe light is turned on and off smoothly to avoid noise contributions at 322kHz. b) shows κ^2 for a varied number of atoms and a light power $P = 5mW$, in c) the corresponding decay constants γ_{extra} and γ_s are shown. In d) the scaling of the normalized atomic noise over N is shown.

For the measurement of $\langle q_{c,s}^{1st} \rangle$, a $\frac{\lambda}{4}$ -plate is inserted in the detection path to switch to a S_3 measurement [67].

In Fig. 5 measurements of κ^2 are shown for different numbers of atoms N with a fixed probe power of 5mW and a probe duration of 1ms. N is varied by changing the temperature of the atomic ensemble. It can be monitored by sending a weak linearly polarized probe beam in the direction of the macroscopic orientation. Due to the Faraday effect the light polarization is rotated by $\theta \propto J_x$ and for the CSS $J_x \approx 4 \cdot N$. The orientation of the atomic ensembles can be tested via magneto optical resonance spectroscopy [68]. Orientations of 0.997(3) are reached regularly in this experimental setup. Fig. 5c displays how the measured decay rate $\gamma = 1/T_2$ can be decomposed in γ_s and γ_{extra} . Clearly $\gamma_s \propto P \cdot \theta_F$.

D. PN measurement

When the coupling constant is known, Eq. (9) can be used to reconstruct the collective atomic operator noise from measurements of noise on $y_{c,s-}$ of the outgoing light. In Fig. 5d measurements of the atomic noise in units of projection noise (PN) are shown for different N . There is a small additional noise component, probably arising from technical noise, which scales with the number of atoms. Only a small range of θ_F and thus N is shown. For higher N additional classical noise of unknown origin is measured, disqualifying higher atomic densities as a working point for quantum noise limited measurements in this setup.

To find the time evolution of the atomic noise, while probe light is present (as the curves shown in Fig. 3a),

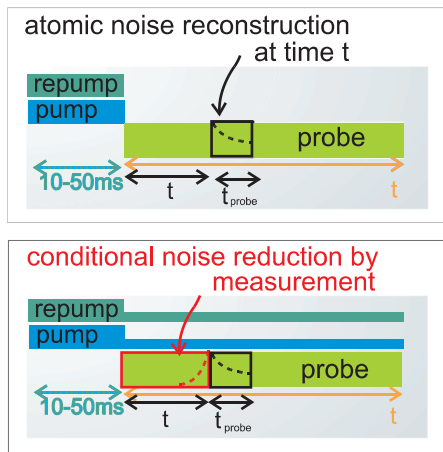


FIG. 6: Pulse sequences for long probe durations. On the left a pulse sequence with a long probe pulse is depicted, displaying the evaluation time interval $[t; t_{\text{probe}}]$ used to find the atomic noise at time t . On the right it is shown how a measurement prior to t can be used to conditionally reduce the atomic noise. For measurements like this typically a fast exponentially growing mode function is used.

$y_{c,s-}$ is evaluated in the time-interval $[t, t+t_{\text{probe}}]$, where t_{probe} is the evaluation time with $\kappa(t_{\text{probe}})$, to find the atomic variances at time t . The corresponding pulse sequence is shown on the left of Fig. 6.

E. Measurement of the conditional atomic noise variance

The theoretical background for generation of the steady state of atoms with the noise reduced by combining dissipation with the measurement is described in Sec. IV. The experimental procedure for the generation of a state with reduced conditional noise variance is described in the following. We wish to squeeze the atomic variances at time t by measuring the outgoing light operators y_c and y_s for the preceding time. The time sequence is illustrated on the right of Fig. 6. The probe pulse is divided in sections, where measurements in the first time interval $[0, t]$ are used for the conditional noise reduction of the atomic operators at time t , and the consecutive time slice $[t, t+t_{\text{probe}}]$ is used for the reconstruction of the atomic state as described above. Here, the quantity of interest is the conditionally reduced atomic variance at time t : $\text{var}(P_{c/s}^{\text{out}})_{\text{con}} = \text{var}(P_{c/s}^{\text{out}} - \alpha y_{c/s}^{\text{probe}}) = \text{var}(\frac{1}{\sqrt{2}J_x}(J_{y,z,I} \pm J_{y,z,II}) - \alpha \frac{1}{\sqrt{2\phi_{\text{probe}}}} S_{2c/s}^{\text{probe}})$ (compare Eq. 5). The superscript "probe" refers to the first time slice from 0 to t . To achieve an optimal noise reduction, α and the temporal mode function of the probe section are optimized. The optimized mode function is exponentially rising with a rate that is typically faster than $1/T_2$. This means that only the last bit of the long preceding pulse is used for the conditional noise reduction. This

behavior is rooted in the additional decoherence mechanisms. The atomic state acquires a noise component piling up with rate γ_{extra} . The measurements closest in time to the atomic state which one wishes to squeeze, should be weighted most.

The actual measurement of $\text{var}(P_{c/s}^{\text{out}})_{\text{con}}$ is done by evaluating $y_{c/s}^{\text{out}}$ in the second time slice $[t; t+t_{\text{probe}}]$. The same reconstruction mechanism as for the unconditional atomic state reconstruction is used, therefore is the second time slice evaluated with an exponentially falling mode function with $\gamma = \gamma_s + \gamma_{\text{extra}}$. Again $\text{var}(y_{c/s-}^{\text{out}})$ is utilized to establish the value of $\text{var}(P_{c/s}^{\text{out}})$ at time t . Accordingly, $\text{var}(y_{c/s}^{\text{out}})_{\text{con}} = \text{var}(y_{c/s-}^{\text{out}} - \alpha^* y_{c/s}^{\text{probe}})$ can be used to find $\text{var}(P_{c/s}^{\text{out}})_{\text{con}}$ with the same reconstruction procedure. The conditional variance can be extracted from the two-time correlation functions $\langle y_{c/s-}^{\text{probe}} y_{c/s-}^{\text{out}} \rangle$: $\sigma_{\text{cond,out}}^2 = \text{var}(y_{c/s-}^{\text{out}}) + \alpha^{*2} \text{var}(y_{c/s}^{\text{probe}}) - 2\alpha^* \langle y_{c/s}^{\text{probe}} y_{c/s-}^{\text{out}} \rangle$ by optimizing α^* , this is assuming that there are no correlations between the light operators at different points in time $\langle y(t)y(t') \rangle = \delta(t-t')$.

VI. CONCLUSIONS

The method discussed in this article allows one to deterministically generate entangled states between two atomic ensembles over a macroscopic distance. The desired quantum state is thereby stabilized by the dissipative mechanism, which renders the created entanglement robust and long-lived. Purely dissipative entanglement generation does not require postselection nor conditioning.

For two-level systems, the dissipative mechanism explained in Sec. III can be used to produce steady state entanglement, i.e. entanglement which is available permanently. This is even possible in the presence of imperfections and noise sources. The use of atoms with a multi-level ground state complicates the generation of steady state entanglement since atoms can undergo transitions to internal levels, which are not coupled to the engineered dynamics in the desired way. Atoms with a two-level ground state such as Ytterbium (^{171}Yb) appear therefore best suited for the realization of the discussed scheme. However, steady state entanglement can also be created in ensembles of atoms with a multilevel structure if strong pumping fields are applied, which transfer the atoms (incoherently) back to a specific two-level sub-system. However, this strategy requires a high optical depth of the atomic sample, or the use of a low finesse cavity. Therefore, a hybrid solution has been implemented in [1], which combines the dissipative mechanism with measurements. As explained in Sec. IV, measurements on the light field yield information on the atomic state and can therefore be used to obtain a quantum state of higher purity and accordingly produce higher entangled states.

The mechanism considered here is applicable in any system which can be coupled to two photonic sideband modes according through a tunable quadratic interaction, for example for the generation of entanglement between two mechanical oscillators. Even though the limited coherence times of quantum systems impose typically severe restrictions on the life times of quantum superposition states, dissipative methods for quantum state engineering allow one to produce event-ready quantum states for applications in Quantum Information Science. Exploring and exploiting all advantages of dissipative approaches will require both, devising new protocols which are capable of generating and processing steady states as well as finding realistic and practical ways of implementing the required coupling of physical systems to a bath.

Acknowledgements

We acknowledge funding by DARPA through the QuSAR program and the EU projects MALICIA, Q-ESSENCE and QUEVADIS. C.A.M. acknowledges support from the Alexander von Humboldt Foundation and the Elite Network of Bavaria (ENB) project QCCC.

Appendix A: Derivation of the master equation

The interaction of atoms and light illustrated in Fig. 1 can be described by the effective ground state Hamiltonian

$$H = H_A + H_L + H_{\text{int}},$$

where excited states have been eliminated using the fact that the detuning $|\Delta|$ is large compared to the Doppler width δ_{Doppler} and atomic decay rates Γ_{atomic} . Here and in the following, Γ_{atomic} denotes the largest effective rate for atomic ground states including single particle as well as collective rates (see below). $H_A = \Omega(J_{x,I} - J_{x,II})$ accounts for the Zeeman splitting of the atoms in the external magnetic field and $H_L = \int dk \omega_k a_{\mathbf{k}}^\dagger a_{\mathbf{k}}$ is the free Hamiltonian of the light field, where $a_{\mathbf{k}}$ is the annihilation operator of a photon with wave vector \mathbf{k} and frequency ω_k . In a rotating frame, the interaction Hamiltonian is given by

$$\begin{aligned} H_{\text{int}} = & \int_{\Delta\omega_{ls}} d\mathbf{k} \sum_{\lambda_{\mathbf{k}}} g(\mathbf{k}) \left(\mu \sum_{i=1}^N \sigma_{I,i} e^{i\Delta\mathbf{k}\mathbf{r}_i} - \nu \sum_{j=1}^N \sigma_{II,j} e^{i\Delta\mathbf{k}\mathbf{r}_j} \right) a_{\mathbf{k}}^\dagger \\ & + \int_{\Delta\omega_{us}} d\mathbf{k} \sum_{\lambda_{\mathbf{k}}} g(\mathbf{k}) \left(\mu \sum_{i=1}^N \sigma_{II,i}^\dagger e^{i\Delta\mathbf{k}\mathbf{r}_i} - \nu \sum_{j=1}^N \sigma_{I,j}^\dagger e^{i\Delta\mathbf{k}\mathbf{r}_j} \right) a_{\mathbf{k}}^\dagger \\ & + H.C., \end{aligned} \quad (\text{A1})$$

where $\lambda_{\mathbf{k}}$ specifies the the two orthogonal polarizations of the light mode with wave vector \mathbf{k} . The first and

second integral cover narrow bandwidths $\Delta\omega_{ls}$ and $\Delta\omega_{us}$ centered around the lower and upper sideband respectively. The atomic operator $\sigma_{I/II,i} = |\uparrow\rangle_{I/II,i} \langle\downarrow|$ refers to a particle in ensemble I/II at position \mathbf{r}_i , $\Delta\mathbf{k} = \mathbf{k}_L - \mathbf{k}$ and \mathbf{k}_L is the wavevector of the applied classical field. $g(\mathbf{k})\mu$ and $g(\mathbf{k})\nu$ denote the effective coupling strengths of the passive (beam splitter-like) part of the interaction and the active (squeezing) component of the Hamiltonian respectively. The laser field covers a very narrow bandwidth around the central frequency ω_L and is sufficiently off-resonant such that the interaction is well within the dispersive regime and absorption effects can be neglected.

Starting from Hamiltonian (A1), a master equation of Lindblad form can be derived for the reduced atomic density matrix $\rho(t)$. To this end, the Born Markov approximation is used, which is well justified for optical frequencies. Since the Larmor splitting exceeds well atomic decay rates $\Omega \gg \Gamma_{\text{atomic}}$, the two sideband modes can be treated as independent baths. The effect of atomic motion gives rise to noise terms and can be included in the master equation in the form of averaged coefficients, where the average in time corresponds to an average in space. This is legitimate in the fast motion limit, where the time scale set by the average velocity of the atoms v is fast compared to the time scale of the radiative decay $\Gamma_{\text{atomic}} \frac{L}{v} \ll 1$. In this case, the emission of light can be described independently of the evolution of atomic positions.

Using the definitions

$$\begin{aligned} A &= \mu \frac{1}{\sqrt{N}} \sum_{i=1}^N \sigma_{I,i} - \nu \frac{1}{\sqrt{N}} \sum_{i=1}^N \sigma_{II,i}, \\ B &= \mu \frac{1}{\sqrt{N}} \sum_{i=1}^N \sigma_{II,i}^\dagger - \nu \frac{1}{\sqrt{N}} \sum_{i=1}^N \sigma_{I,i}^\dagger, \end{aligned}$$

the resulting master equation can be cast in the form

$$\begin{aligned} \frac{d}{dt} \rho(t) = & \frac{1}{2} d\Gamma A \rho(t) A^\dagger + \frac{1}{2} d\Gamma B \rho(t) B^\dagger \\ & + \frac{1}{2} \Gamma \mu^2 \sum_{i=1}^N \left(\sigma_{I,i} \rho(t) \sigma_{I,i}^\dagger + \sigma_{II,i}^\dagger \rho(t) \sigma_{II,i} \right) \\ & + \frac{1}{2} \Gamma \nu^2 \sum_{i=1}^N \left(\sigma_{I,i}^\dagger \rho(t) \sigma_{I,i} + \sigma_{II,i} \rho(t) \sigma_{II,i}^\dagger \right) \\ & + \dots, \end{aligned} \quad (\text{A2})$$

where Γ is the single particle decay rate and a short hand notation was used. Master equations of Lindblad form $\frac{d}{dt} \rho(t) = \frac{\gamma}{2} (A \rho(t) A^\dagger - A^\dagger A \rho(t)) + H.C.$ with decay rate γ and jump operator A are abbreviated by the expression $\frac{d}{dt} \rho(t) = \frac{\gamma}{2} A \rho(t) A^\dagger + \dots$. d denotes the resonant optical depth of one atomic ensemble. Note that the entangling terms in the first line are enhanced

by a factor d , such that for sufficiently optically thick samples, the additional noise terms reflecting thermal motion are small compared to the desired contributions.

Next, additional cooling and heating processes, as well as dephasing are included. The full master equation is given by

$$\begin{aligned} \frac{d}{dt} \rho(t) = & \frac{1}{2} d \Gamma A \rho(t) A^\dagger + \frac{1}{2} d \Gamma B \rho(t) B^\dagger \\ & + \frac{1}{2} \Gamma_{\text{cool}} \sum_{i=1}^N \left(\sigma_{I,i} \rho(t) \sigma_{I,i}^\dagger + \sigma_{II,i}^\dagger \rho(t) \right) \\ & + \frac{1}{2} \Gamma_{\text{heat}} \sum_{i=1}^N \left(\sigma_{I,i}^\dagger \rho(t) \sigma_{I,i} + \sigma_{II,i} \rho(t) \sigma_{II,i}^\dagger \right) \\ & + \frac{1}{2} \Gamma_{\text{deph}} \sum_{i=1}^N \left(\sigma_{\downarrow\downarrow,I,i} \rho(t) \sigma_{\downarrow\downarrow,I,i} + \sigma_{\downarrow\downarrow,II,i} \rho(t) \sigma_{\downarrow\downarrow,II,i} \right), \\ & + \dots, \end{aligned} \quad (\text{A3})$$

with $\sigma_{\uparrow\uparrow,I/II,i} = |\uparrow\rangle_{I/II,i} \langle\uparrow|$ and $\sigma_{\downarrow\downarrow,I/II,i} = |\downarrow\rangle_{I/II,i} \langle\downarrow|$. The noise terms proportional to $\Gamma\mu^2$ and $\Gamma\nu^2$ in Eq. (A2) have been absorbed in the second and third line of Eq. (A3) respectively. The last three lines represent single particle processes. Hence they do not feature a collective enhancement factor as the entangling terms in the first line. As shown in [3], Eq. (A3) includes all terms that need to be taken into account. Collective dephasing terms, as well as collective contributions due to pump and repump fields can be neglected. Similarly, the distance R between the two ensembles does not play a role for $k_L \gg R/L^2$ and $k_L L \gg 1$, where L is the spatial extend of an atomic ensemble. For the experimental setting under consideration this condition is fulfilled.

Appendix B: Calculation of entanglement

Below it is shown how the entanglement measured by the quantity $\xi = \Sigma_J / (2|\langle J_x \rangle|)$, where $\Sigma_J = \text{var}(J_{y,I} - J_{y,II}) + \text{var}(J_{z,I} - J_{z,II})$, can be determined in the limit $N \gg 1$, assuming that the number of atoms in the two-level system N_2 depends on time. For clarity, operators referring to the two-level model are labelled with subscript "2". The time derivative of the variance Σ_{J_2} is calculated using Eq. (A3). By applying the decorrelation approximation $\langle J_{y/z}(t) J_x(t) \rangle_2 \approx \langle J_{y/z}(t) \rangle_2 \langle J_x(t) \rangle_2$ for mean values of products of transverse and longitudinal spins one obtains

$$\begin{aligned} \frac{d}{dt} \Sigma_{J_2}(t) = & - \left(\tilde{\Gamma} + d(t) \Gamma P_2(t) \right) \Sigma_{J_2}(t) \\ & + N_2(t) \left(\tilde{\Gamma} + d(t) \Gamma P_2(t) \right)^2 (\mu - \nu)^2, \end{aligned}$$

where $d(t) = d N_2(t)/N$, $\tilde{\Gamma} = \Gamma_{\text{cool}} + \Gamma_{\text{heat}} + \Gamma_{\text{deph}}$ and $P_2(t) = 2\langle J_x(t) \rangle / (N_2(t))$. For $t \rightarrow \infty$ and $N_2 = N$,

$$\Sigma_{J_2,\infty} = N \frac{\tilde{\Gamma} + d \Gamma P_{2,\infty}^2 (\mu - \nu)^2}{\tilde{\Gamma} + d \Gamma P_{2,\infty}}.$$

Next, the time evolution of the longitudinal spin is considered. Eq. (A3) yields

$$\begin{aligned} \frac{d}{dt} \langle J_x(t) \rangle_2 = & - (\Gamma_{\text{heat}} + \Gamma_{\text{cool}}) \langle J_x(t) \rangle_2 \\ & + \frac{N_2(t)}{2} (\Gamma_{\text{cool}} - \Gamma_{\text{heat}}), \end{aligned}$$

such that for constant particle number $N_2 = N$,

$$\langle J_x \rangle_{2,\infty} = \frac{N}{2} \frac{\Gamma_{\text{cool}} - \Gamma_{\text{heat}}}{\Gamma_{\text{cool}} + \Gamma_{\text{heat}}},$$

and therefore

$$\xi_{2,\infty} = \frac{1}{P_{2,\infty}} \frac{\tilde{\Gamma} + d \Gamma P_{2,\infty}^2 (\mu - \nu)^2}{\tilde{\Gamma} + d \Gamma P_{2,\infty}}, \quad (\text{B1})$$

$$P_{2,\infty} = \frac{\Gamma_{\text{cool}} - \Gamma_{\text{heat}}}{\Gamma_{\text{cool}} + \Gamma_{\text{heat}}} \quad (\text{B2})$$

in the steady state. In the limit $d \rightarrow \infty$, this equation reduces to $\xi_{2,\infty} = (\mu - \nu)^2$.

The variation of $N_2(t)$ and $P_2(t)$ is slow compared to the evolution of $\Sigma_{J_2}(t)$. In the limit where the entangled quantum state follows the changing particle number and atomic polarization adiabatically, $\xi_2(t)$ is given by

$$\begin{aligned} \xi_2(t) = & \frac{\Sigma_{J_2}(0)}{2P_2(t)} e^{-(\tilde{\Gamma} + d(t) \Gamma P_2(t))t} \\ & + \frac{\tilde{\Gamma} + d(t) \Gamma P_2(t)^2 (\mu - \nu)^2}{P_2(t) (\tilde{\Gamma} + d(t) \Gamma P_2(t))} \left(1 - e^{-(\tilde{\Gamma} + d(t) \Gamma P_2(t))t} \right). \end{aligned} \quad (\text{B3})$$

Appendix C: Towards purely dissipative steady state entanglement using incoherent pump fields

In the following, we explain how the estimates shown in Fig. 3b are obtained. We use here a simplified model, which has been employed in [1] to compare the measured results to the theoretical predictions. Details regarding these fits can be found in the Supplemental Material of [1]. We model the experiment in terms of three atomic levels $|\uparrow\rangle_I \equiv |4, 4\rangle_I$, $|\downarrow\rangle_I \equiv |4, 3\rangle_I$ and $|h\rangle_I \equiv |3, 3\rangle_I$ ($|\uparrow\rangle_{II} \equiv |4, -3\rangle_{II}$, $|\downarrow\rangle_{II} \equiv |4, -4\rangle_{II}$ and $|h\rangle_{II} \equiv |3, -3\rangle_{II}$) for the first (second) ensemble. For the timescales considered here, the atomic population in other internal states is negligible. In order to describe the underlying physics qualitatively, using only a small number of parameters, we assume further that $\Gamma_{|4,\pm 4\rangle \rightarrow |h\rangle} \approx \Gamma_{|4,\pm 3\rangle \rightarrow |h\rangle} = \Gamma_{\text{out}}$ and $\Gamma_{|h\rangle \rightarrow |4,\pm 4\rangle} \approx \Gamma_{|h\rangle \rightarrow |4,\pm 3\rangle} = \Gamma_{\text{in}}$, where the abbreviations $\Gamma_{|4,\pm 4\rangle \rightarrow |4,\pm 3\rangle} = \Gamma_{4,3}$ and $\Gamma_{|4,\pm 3\rangle \rightarrow |3,\pm 4\rangle} = \Gamma_{3,4}$

have been used.

Atomic transitions are taken into account by introducing the collisional rate Γ_{col} . Since the atomic thermal energy is large compared to the level splittings, we assume the same rate Γ_{col} for all atomic transitions. Finally, we include σ_{\pm} polarized pump and repump fields, which induce resonant transitions with $\Delta m_F \pm 1$ in the first/second ensemble as shown in Fig. 2b. Pump fields drive transitions within the manifold of atomic states with $F = 4$ and repump fields transfer atoms from states with $F = 3$ back to $F = 4$. In this case,

$$\begin{aligned}\Gamma_{\text{out}} &= \Gamma_{\text{L}}^{\text{out}} + \Gamma_{\text{col}}, \\ \Gamma_{\text{in}} &= \Gamma_{\text{repump}} + \Gamma_{\text{col}}.\end{aligned}$$

where $\Gamma_{\text{L}}^{\text{out}}$ is the rate at which atoms leave the two-level subsystem due to radiative transitions caused by the driving field. Γ_{repump} is the rate at which the applied repump fields transfer atoms back. Transitions within the two-level subsystem occur at the rates

$$\begin{aligned}\Gamma_{3,4} &= \mu^2 \Gamma + \Gamma_{\text{pump}} + \Gamma_{\text{col}}, \\ \Gamma_{4,3} &= \nu^2 \Gamma + \Gamma_{\text{col}}.\end{aligned}$$

$\mu^2 \Gamma$ and Γ_{pump} are the driving field and pump field induced cooling rates respectively. The heating rate caused by the driving field is given by $\nu^2 \Gamma$. Note that the application of pump fields leads to an increased dephasing rate $\tilde{\Gamma}$. In contrast, repump fields do not have an effect on $\tilde{\Gamma}$ [3]. We estimate the effect of these fields on the dephasing rate by adding $2\Gamma_{\text{pump}}$ to $\tilde{\Gamma}$.

Fig. 3b shows the predicted time evolution of entanglement for $d = 55; 100; 150$. The parameters take the values used to fit the experimental data measured in the absence of additional fields (compare Fig. 2, panels a and b in [1]), $\Gamma = 0.002\text{ms}^{-1}$, $\tilde{\Gamma} = 0.193\text{ms}^{-1}$, $\Gamma_{\text{col}} = 0.002\text{ms}^{-1}$ and $Z = 2.5$. The presence of both, pump and repump fields is included as described above with $\Gamma_{\text{pump}} = \Gamma_{\text{repump}} = 0.160\text{ms}^{-1}$.

-
- [1] H. Krauter, C.A. Muschik, K. Jensen, W. Wasilewski, J.M. Petersen, J.I. Cirac, E.S. Polzik, Phys. Rev. Lett. **107**, 080503 (2011).
- [2] H. Krauter, C.A. Muschik, K. Jensen, W. Wasilewski, J.M. Petersen, J.I. Cirac, E.S. Polzik, arXiv:1006.4344 (2010).
- [3] C.A. Muschik, E.S. Polzik, J.I. Cirac, Phys. Rev. A **83**, 052312 (2011).
- [4] A.S. Parkins, E. Solano, and I.J. Cirac, Phys. Rev. Lett. **96**, 053602 (2006).
- [5] J.F. Poyatos, J.I. Cirac and P. Zoller, Phys. Rev. Lett. **77**, 4728 (1996).
- [6] J.P. Paz and W. H. Zurek, Proc. R. Soc. A, **454**, 355 (1998).
- [7] M.B. Plenio, S.F. Huelga, A. Beige, and P.L. Knight, Phys. Rev. A, **59**, 2468 (1999).
- [8] A. Beige, D. Braun, B. Tregenna, and P.L. Knight, Phys. Rev. Lett. **85**, 1762 (2000).
- [9] M.B. Plenio and S.F. Huelga, Phys. Rev. Lett. **88**, 197901 (2002).
- [10] B. Kraus and J.I. Cirac, Phys. Rev. Lett. **92**, 013602 (2004).
- [11] R. Guzmán, J. C. Retamal, E. Solano, and N. Zagury, Phys. Rev. Lett. **96**, 010502 (2006).
- [12] F. Dimer, B. Estienne, A.S. Parkins, and H. J. Carmichael, Phys. Rev. A **75**, 013804 (2007).
- [13] S. Diehl, A. Micheli, A. Kantian, B. Kraus, H.P. Büchler, P. Zoller, Nature Physics **4**, 878 (2008).
- [14] B. Kraus, H.P. Büchler, S. Diehl, A. Kantian, A. Micheli, and P. Zoller, Phys. Rev. A **78**, 042307 (2008).
- [15] F. Verstraete, M.M. Wolf, J.I. Cirac, Nature Physics **5**, 633 (2009).
- [16] R. Bloomer, M. Pysher and O. Pfister, New J. Phys. **13**, 063014 (2011).
- [17] D.G. Angelakis, L. Dai and L.-C. Kwek, Europhys. Lett. **91** 10003 (2010).
- [18] J. Kerckhoff, H.I. Nurdin, D.S. Pavlichin, and H. Mabuchi, Phys. Rev. Lett. **105**, 040502 (2010).
- [19] G.X. Li and Z. Ficek, Optics Commun. **283**, 814 (2010).
- [20] F. Pastawski, L. Clemente, and J.I. Cirac, Phys. Rev. A **83**, 012304 (2011).
- [21] J. Cho, S. Bose, and M.S. Kim, Phys. Rev. Lett. **106**, 020504 (2011).
- [22] J.T. Barreiro, M. Müller, P. Schindler, D. Nigg, T. Monz, M. Chwalla, M. Hennrich, C.F. Roos, P. Zoller, and R. Blatt, Nature **470**, 486 (2011).
- [23] F. Queisser, T. Zell and R. Klesse, arXiv:1111.5531 (2011).
- [24] M.J. Kastoryano, F. Reiter, and A.S. Sørensen, Phys. Rev. Lett. **106**, 090502 (2011).
- [25] M. Kliesch, T. Barthel, C. Gogolin, M. Kastoryano, and J. Eisert, Phys. Rev. Lett. **107** 120501 (2011).
- [26] M. Kiffner and U. Dorner and D. Jaksch, arXiv:1112.3885 (2011).
- [27] Note that the term "entanglement between macroscopic objects" does not refer to a macroscopic superposition since the generated entanglement corresponds to less than one e-bit.
- [28] L.M. Duan, J.I. Cirac, P. Zoller and E.S. Polzik, Phys. Rev. Lett. **85**, 5643 (2000).
- [29] B. Julsgaard, J. Sherson, J.I. Cirac, J. Fiurášek, E.S. Polzik, Nature **432**, 482 (2004).
- [30] J. Sherson, A.S. Sørensen, J. Fiurášek, K. Mølmer, and E.S. Polzik, Phys. Rev. A **74** 011802 (2006).
- [31] J. Sherson, B. Julsgaard and E.S. Polzik, Advances in Atomic, Molecular, and Optical Physics, **54** (2006).
- [32] J.F. Sherson, H. Krauter, R.K. Olsson, B. Julsgaard, K. Hammerer, I. Cirac, E.S. Polzik, Nature **443**, 557

- (2006).
- [33] K. Hammerer, A. S. Sørensen, E. S. Polzik, *Rev. Mod. Phys.* **82**, 1041 (2010).
- [34] K. Jensen, W. Wasilewski, H. Krauter, T. Fernholz, B.M. Nielsen, M. Owari, M.B. Plenio, A. Serafini, M.M. Wolf, E.S. Polzik, *Nature Phys.* **7**, 13 (2010).
- [35] C.A. Muschik, H. Krauter, K. Hammerer and E.S. Polzik, *Quantum Inf. Process.* **10**, 839 (2011).
- [36] C.A. Muschik, K. Hammerer, E.S. Polzik, and J.I. Cirac, *Phys. Rev. A* **73**, 062329 (2006).
- [37] J. Fiurášek, J. Sherson, T. Opatrný, and E.S. Polzik, *Phys. Rev. A* **73**, 022331 (2006).
- [38] K.G.H. Vollbrecht, C.A. Muschik and J.I. Cirac, *Phys. Rev. Lett.* **107**, 120502 (2011).
- [39] A. Einstein, B. Podolsky and N. Rosen, *Phys. Rev.* **47**, 777 (1935).
- [40] In the famous example introduced by Einstein, Podolski and Rosen, the quantum state under consideration is a simultaneous eigenstate of the sum of positions $x_+ = x_I + x_{II}$ and difference of momenta $p_- = p_I - p_{II}$ of two separate particles. This corresponds to an infinitely squeezed state with $\text{var}(x_+) = \text{var}(p_-) = 0$, where the momenta/positions are perfectly correlated/anticorrelated.
- [41] S.L. Braunstein and P. van Loock, *Rev. Mod. Phys.* **77**, 513 (2005).
- [42] M.G. Raymer, A.C. Funk, B.C. Sanders, and H. de Guise, *Phys. Rev. A* **67**, 052104 (2003).
- [43] B. Julsgaard, A. Kozhekin, and E.S. Polzik, *Nature* **431**, 400 (2001).
- [44] ^{133}Cs is an alkali atom with nuclear spin $I = 3/2$. The ground state is split into two manifolds with total spin $F = I \pm 1/2$.
- [45] L.-M. Duan, M. D. Lukin, J. I. Cirac and P. Zoller, *Nature* **414**, 413 (2001).
- [46] T. Chanelière, D. N. Matsukevich, S. D. Jenkins, S.-Y. Lan, T.A.B. Kennedy and A. Kuzmich, *Nature* **438**, 833 (2005).
- [47] C.W. Chou, H. de Riedmatten, D. Felinto, S.V. Polyakov, S.J. van Enk, and H. J. Kimble, *Nature* **438**, 828 (2005).
- [48] M.D. Eisaman, A. André, F. Massou, M. Fleischhauer, A.S. Zibrov and M.D. Lukin, *Nature* **438**, 837 (2005).
- [49] D.N. Matsukevich, T. Chanelière, S.D. Jenkins, S.-Y. Lan, T.A.B. Kennedy, and A. Kuzmich, *Phys. Rev. Lett.* **96**, 030405 (2006).
- [50] K.S. Choi, H. Deng, J. Laurat, and H.J. Kimble, *Nature* **452**, 67 (2008).
- [51] Z.-S. Yuan, Y.-A. Chen, B. Zhao, S. Chen, J. Schmiedmayer, and J.-W. Pan, *Nature* **454**, 1098 (2008).
- [52] Y.-A. Chen, S. Chen, Z.-S. Yuan, B. Zhao, C.-S. Chuu, J. Schmiedmayer, and J.-W. Pan, *Nature Phys.* **4** 103 (2008).
- [53] H. J. Kimble, *Nature* **453**, 1023 (2008).
- [54] A measurement yielding the result e , produces the quantum state ρ_e . The situation where no measurement is performed corresponds to the situation where the measurement result is unknown. The resulting mixed state is given by $\tilde{\rho} = \sum_e P(e)\rho_e$, where $P(e)$ is the probability to obtain the measurement result e and the sum \sum_e runs over all possible measurement results.
- [55] In the experiment reported on here, the light field is measured continuously due to technical reasons. However, the measurement results are not used in the first set of experiments, where entanglement is created purely dissipatively. This corresponds to a situation where the measurement outcomes are not known or, equivalently, no measurement is performed.
- [56] M. Takeuchi, T. Takano, S. Ichihara, Y. Takasu, M. Kumakura, T. Yabuzaki and Y. Takahashi, *Appl. Phys. B* **83** 107 (2006).
- [57] T. Takano, M. Fuyama, R. Namiki, and Y. Takahashi, *Phys. Rev. Lett.* **102**, 033601 (2009).
- [58] T. Holstein and H. Primakoff, *Phys. Rev.* **58**, 1098 (1940).
- [59] A. Silberfarb and I.H. Deutsch, *Phys. Rev. A* **68**, 13817 (2003).
- [60] L.B. Madsen and K. Mølmer, *Phys. Rev. A* **70**, 52324 (2004).
- [61] K. Hammerer, E. S. Polzik and J. I. Cirac, *Phys. Rev. A* **72**, 052313 (2005).
- [62] G. Giedke, G. and J.I. Cirac, *Phys. Rev. A* **66**, 032316 (2002).
- [63] In this case the Hamiltonian is given by $H = H_c + H_s$, where $H_{c/s} = H_{c/s}^{\text{ent}} + H_{c/s}^{\text{noise}}$. $H_{c/s}^{\text{ent}} = \sqrt{2}\gamma_s (\frac{1}{Z} X_{c/s} y_{c/s} + Z P_c q_{c/s})$ corresponds to the desired entangling interaction, while $H_{c/s}^{\text{noise}} = \sqrt{2}\gamma_{\text{extra}} (X_{c/s} x_{N,c/s} + P_{c/s} p_{N,c/s})$ describes transverse dephasing at a rate γ_{extra} . $x_{N,c/s}$ and $p_{N,c/s}$ refer to noise modes with $\langle x_{N,c/s}(t) \rangle = \langle p_{N,c/s}(t) \rangle = 0$, $\langle x_{N,c/s}(t) x_{N,c/s}(t') \rangle = \langle p_{N,c/s}(t) p_{N,c/s}(t') \rangle = \delta(t - t')/2$ and $[x_{N,c/s}, p_{N,s/c}] = 0$.
- [64] Note that the exponentially growing and falling modes are not orthogonal. Taking this into account: $U^2 = \epsilon^4 + e^{-2T\gamma} (-1 + \epsilon^2)^2 - 2\sqrt{e^{-2T\gamma} T\gamma \epsilon^2 (-1 + \epsilon^2)} \text{Csch}(T\gamma)$ and $V^2 = \frac{e^{-2T\gamma} \epsilon^2 (-1 + \epsilon^2) (-1 - e^{-2T\gamma} + 2e^{2T\gamma} \sqrt{e^{-2T\gamma} T\gamma} \text{Csch}(T\gamma))}{\xi^2} \approx 0$. ϵ^2 can be easily extracted from κ^2 : $\epsilon^2 = (1 - \kappa^2)/(1 - e^{-2T/T^2})/Z^2$
- [65] W. Wasilewski, K. Jensen, H. Krauter, J.J. Renema, M.V. Balabas, and E. S. Polzik, *Phys. Rev. Lett.* **104**, 133601 (2010).
- [66] J. Sherson, PhD thesis: "Quantum memory and teleportation using macroscopic gas samples", University of Aarhus (2006). <http://www.nbi.dk/~sherson/thesis.pdf>
- [67] To test if the measurement is set up correctly, one creates a fixed signal coming from the atoms in one atomic ensemble e.g. created by a magnetic RF pulse. Following Eq. 4, the atomic signal should be suppressed by $1/Z^2$ in a $\langle S_3 \rangle$ - compared to a $\langle S_2 \rangle$ -measurement.
- [68] B. Julsgaard, J. Sherson, J.L. Soerensen, and E.S. Polzik, *Journal of Optics B* **6**, 5 (2004).